

An Assessment of the NASA Flammability Screening Test and Related Aspects of Material Flammability

Thomas J. Ohlemiller
Building and Fire Research Laboratory
Gaithersburg, MD 20899

August 1992
Order #C-32003-R



Prepared for:
National Aeronautics and Space Administration
Lewis Research Center
Cleveland, Ohio 44135

U.S. Department of Commerce
Barbara Hackman Franklin, *Secretary*
Technology Administration
Robert M. White, *Under Secretary for Technology*
National Institute of Standards and Technology
John W. Lyons, *Director*

Table of Contents

	Page
List of Tables	iv
List of Figures	v
Abstract	1
1. Chapter One	2
Summary of the NASA Flammability Test Assessment	
2. Chapter Two	6
One and Two-Sided Burning of Thermally-Thin Materials	
3. Chapter Three	18
Design of an Experiment to Demonstrate the Effects of Self-Feedback of Radiation on Flamespread Behavior	
4. Chapter Four	22
Conclusions and Recommendations from this Study	
5. Acknowledgements	23
References	24

List of Tables

	Page
Table 1.	
Description of Test Materials in One vs Two-Sided	
Burning Study	25

List of Figures

	Page
Figure 1. Steady-State Model, Result One and Two-Sided Heating/Burning	26
Figure 2. Transient Model Result, One-Sided Heating/Burning	27
Figure 3. Transient Model Result, One-Sided Heating/Burning	28
Figure 4. Transient Model Result, One-Sided Heating/Burning	29
Figure 5. Transient Model Result, Effect of Activation Energy on Rate of Heat Release	30
Figure 6. Transient Model Result, One-Sided and Two-Sided Heating/ Burning	31
Figure 7. Apparatus for One and Two-Sided Burning of Samples in the Cone Calorimeter	32
Figure 8. Haysite H755 One-sided Irradiance at 18kW/m^2	33
Figure 9. One-Sided and Two-Sided Rate of Heat Release G-11 Epoxy/Glass, 1.5 mm Thick	34
Figure 10. One-Sided and Two-Sided Rate of Heat Release Haysite H755 Polyester/Glass, 1.5 mm Thick	35
Figure 11. One-Sided and Two-Sided Rate of Heat Release Haysite ETS Polyester/Glass, 1.5 mm Thick	36
Figure 12. Centerline View Factor Dependence on Ratio of Source Size to Gap Width	37
Figure 13. Variation of Local View Factor with Ratio of Source Width to Gap	38
Figure 14. Elements of Apparatus to Examine Radiation Self-Feedback Effect on Opposed-Flow Flame Spread	39

An Assessment of the NASA Flammability Screening Test and Related Aspects of Material Flammability

T. J. Ohlemiller
Building & Fire Research Laboratory

Abstract

This final report summarizes the results of an assessment of the NASA flammability screening test (8060.1B) for materials to be used in manned spacecraft interiors. A set of materials was examined using the standard NASA test, a modified version of this test which incorporated external radiation and NIST tests which measure ignitability, rate of heat release and opposed flow flame spread behavior. Materials passing the standard NASA screening test showed widely varying degrees of flammability enhancement when subjected to external radiation (modified NASA test, NIST tests). Since such radiation is implicit in many normal fire scenarios, materials passing the standard NASA screening test should not be treated as non-flammable. The quantitative role of self-feedback of radiation remains to be fully clarified; an apparatus to examine this issue was built but no tests could be completed in the allotted time. The rate of heat release from the two-sided burning of thermally-thin materials was quantitatively compared to that for one-sided burning; this issue was believed to be at the heart of certain anomalies in the earlier stages of this study. A synergistic enhancement of heat release rate was indeed found for two-sided burning of three materials; two simplified models account for the origin of this effect. On the basis of this study, it is recommended that NASA supplement their existing flammability screening test with one that incorporates external radiation. It is further recommended that this supplemental test in normal gravity be correlated experimentally with a similar test in micro-gravity.

Chapter One

Summary of the NASA Flammability Test Assessment*

Two types of questions have been raised concerning the screening test (8060.1B) which NASA uses to assess the flammability of materials that might be used in spacecraft interiors [1]. This test involves subjecting a material to a well-defined chemical igniter on its bottom edge and determining the extent of upward flame spread.** A material which gives less than 15 cm propagation passes. The first question concerns whether the behavior seen in such a test, carried out necessarily under normal gravity conditions, is inherently worse than would be seen in micro-gravity conditions. The indication that this could be so came from tests which were done aboard Skylab [2]; in all cases the materials tested there in an oxygen-rich environment, with no gas flow past the sample, yielded slower flame spread rates than in comparable conditions under normal gravity. More recently, Olson, et al [3] have shown that, when there is gas flow past the sample, flame spread on a very thin paper can be faster in micro-gravity than it is in normal gravity. Steinberg [4] also found that some metals can burn more persistently in micro-gravity than in normal gravity. The generality of these results is not clear but they raise serious doubts about the assertion that micro-gravity flammability can safely be assumed to be always less than that in normal gravity. This issue was not addressed in the present study; the facilities to properly address it do not yet exist. In the last Chapter of this report, recommendations are made as to how this problem might be approached.

The present study has addressed the second question regarding the NASA flammability screening test: is this test a worst case test for normal gravity? The assertion that it is derives from the fact that this is an upward spread test. Upward spread, which is one example of concurrent spread (flame spread in the same direction as the gas flow), is more effective in the transfer of heat to adjacent, non-burning elements of a fuel than is opposed flow spread (e. g., lateral spread across a vertical surface, downward spread on a vertical surface). Of all cases driven strictly by buoyant flow, upward spread is almost certainly the worst.

*The reader is referred to Ref. 1 for further details of the NASA flammability test assessment study that is summarized in this chapter.

**The material is to be tested in the highest oxygen level to which it would be exposed in usage, typically 30%. It also is to be tested at its "worst case" thickness, presumably the thinnest contemplated usage.

However, the NASA test lacks a feature now generally included in many other assessments of flammability -- external radiation.

External radiation is recognized as an important determinant of the flammability behavior which a material exhibits. Radiation can play a role in real fires in two possible ways. First, a nearby object may be burning and irradiating the material of interest. Second, the material of interest may have a concave surface, which, if burning, will exchange radiation with itself. Different surface elements having a finite radiative view factor towards each other will interact in this manner.*** With either source of radiation flammability is enhanced in proportion to the heat flux but the response varies with the nature of the material (both its physical and chemical characteristics).

NIST has developed a set of tests to measure the flammability of a material. This flammability is a composite of three aspects of the behavior of a material: ignitability, rate of heat release and flame spread characteristics. The NIST tests measure all of these as a function of external radiant flux; thus ignition delay time decreases with increased flux, rate of heat release (kW/m^2) increases and so also does rate of flame spread (opposed or concurrent flow; the test used here is for opposed flow spread). The results of these tests are reduced to simplified semi-empirical model descriptions of the flux-dependent behavior of the material. These models then become sub-models to describe the behavior of the material in the context of a broader compartment fire model. This approach to flammability recognizes that fire growth on a material can be quite dependent on the scenario in which the material is first exposed to an ignition source. The tests results are certainly dependent on gravity; there is no simple way one could extrapolate the results to a micro-gravity situation.

In the present study a comparison was made, for a series of materials, of the flammability behavior seen in the NASA test and in the above NIST tests. The goal was to see what correlation exists in the behavior exhibited in the two types of flammability measure. In particular, one would like to see that a passing performance in the NASA test also implies a combination of low ignitability, low rate of heat release and slow flame spread even for relatively high radiant fluxes in the NIST tests.

It should be noted that all of the NASA and NIST tests were done in atmospheric air rather than in elevated oxygen. The quantitative results would certainly be affected by increased ambient oxygen but the principal qualitative conclusions should not be.

***A folded surface can have a view factor approaching unity; further discussion of such view factors can be found in Chapter 3 of this report.

The comparison study was actually carried out in two stages. In the first stage all but one of the five sample materials passed the NASA test in air whereas they exhibited a wide variety of behaviors in the NIST tests. The quantifiable aspects of the behavior in the normal NASA test were too limited to facilitate a meaningful search for a correlation with the NIST behavior. It was decided to modify the NASA test by the addition of the one element it lacks, external radiation. A new set of materials, partially overlapping the first set was subjected to this modified NASA test and to the NIST tests with some aspects of the latter also modified to more closely respond to NASA tests (burning without an insulation board in contact with one face of the sample). The comparison thus became the following: extent of upward flame spread as a function of incident heat flux in the modified NASA test, using one and sometimes three NASA igniters to assure sample ignition, versus behavior in the three NIST tests above.

The addition of an external flux in the NASA test had widely varying consequences. One of the materials (a Nomex cloth) required very little external radiation to achieve a full length (30 cm) burn; other materials such as Lexan showed little response to the limited flux level achievable with the available radiant panel.

These materials also showed a wide range of behaviors in the NIST tests but it should be noted that all of the materials burned in these tests. None could be termed "non-flammable".

No simple correlation emerged between the behaviors seen in the two types of flammability testing; reference 1 should be consulted for details. It is probable that no single measure from the NIST tests, such as rate of heat release, should be expected to be an assured predictor of the upward flame spread behavior in the modified NASA test. However, even when indirect measures of flammability from the NIST tests were applied in the context of a semi-empirical, upward flame spread model, the two types of results could not be correlated. One evident conclusion is that our understanding of the varied aspects of the flammability of real materials needs further development.

The more important conclusion has to be that the current usage of a pass/fail criterion in assessing flammability with the standard NASA test is not desirable inasmuch as this leads to a dichotomy in the way materials are subsequently handled. Materials which pass the test (in worst case conditions) are treated as if they are not flammable in expected spacecraft usage. Passage of the standard NASA test clearly does provide some indication of lesser flammability but, as the modified NASA tests and the NIST tests show, passage does not indicate sensitivity to external radiation. Real spacecraft applications of the material could subject it to radiation levels (external or self-feedback) that might substantially enhance its flammability. Acceptability of a material,

particularly a material to be extensively used in a spacecraft, should be judged in light of its response to radiation levels that it may realistically encounter.

The final phase of this study, which is reported in detail in the next two chapters, pursued issues which arose in the preceding work. One reason for the failure of the NIST and modified NASA test results to correlate may lie in the fact that the former involved one-sided burning of the samples while the latter involved two-sided burning. The basis for this possible source of differences is discussed in detail in Chapter 2. The possible crucial role of radiation self-feedback in flammability enhancement has prompted an investigation of its magnitude and actual impact. In Chapter 3 the detailed rationale and design of an experimental apparatus for this purpose is laid out; it has not been possible to carry out the necessary experiments as yet.

Chapter Two

One and Two-Sided Burning of Thermally-Thin Materials

Introduction

In spacecraft applications, many slab-like materials are dimensionally thin as a result of weight considerations. These materials may also be expected to approach thermally-thin behavior during combustion. By thermally-thin is meant that heat absorbed on one surface of the material will penetrate its thickness sufficiently rapidly so that there will be no significant temperature gradient through the material depth. The specific criteria for such behavior are addressed below.

In testing the flammability of a material, it is important to measure the worst behavior it is likely to exhibit in the application of interest. For any application of a slab-like material it is pertinent to ask whether simultaneous burning on both surfaces is possible; this is clearly worse than the burning of one surface only. When this occurs with a dimensionally thick material, the result is a doubling of the burning rate or overall rate of heat release because twice as much surface area is involved. This simple factor of two relation pertains because such dimensionally thick materials typically are also thermally-thick. The heat wave in the material from the burning of each surface does not extend past the center plane through the material. As a result the two burning surfaces are thermophysically isolated and do not interact. (There could be other interactions in a real application, such as competition of the two burning surfaces for the same oxygen supply.) For dimensionally thin materials, the approach to thermally-thin behavior implies just the opposite: the thermal waves from the two burning surfaces merge to the point of producing a uniform temperature through the depth of the material. In this case the thermophysical interaction between the burning zones is a maximum. The heat feedback from the flame on one surface is felt by both burning surfaces and there is an enhancement of the burning rate that is greater than a factor of two. The details behind this are encompassed in the models discussed below. From a fire safety point of view, this means that two-sided burning on thin materials is more hazardous than one might initially expect. Thus any thin material which conceivably could burn on both surfaces in a spacecraft application should be tested in this way (even if such burning would require the failure of some initial bonding to a nominally protective second surface).

The specific application of these ideas in this work has been in the measurement of the rate of heat release from thin materials burning on one or two sides while irradiated in the NIST Cone Calorimeter apparatus. Specific details of that apparatus add certain complications to the measurements, as will be seen. First,

however, the basis for the thermally-thin enhancement of burning rate (or heat release rate) will be examined in the context of two models.

Simplified Models for Burning of Thermally-Thin Materials

Steady-state model. The qualitative essence of the problem can be seen in a simple steady-state energy balance. Consider two different burning conditions for a thermally thin material: 1) the material is irradiated with a constant flux on one surface and is burning on that surface only; 2) the material is irradiated on both surfaces and is burning on both surfaces also. The external radiation is included for the usual reason that it simulates either a nearby burning object or self-feedback of radiation from a burning surface with a concave geometry. In case (1) the material is gasifying from both sides at an equal rate but only half of those gasification products are burning. This is so because the degradation and gasification of the solid fuel is a volumetric process, not a surface process. Since, in a thermally-thin material, the temperature is constant throughout the depth, the gasification rate is also and the products tend to depart equally from both surfaces.

The use of a steady-state argument for a thermally-thin material is an artifice. Fuel depletion is inherently important in such a thin fuel and so the process is necessarily transient. Depletion is included in the second model below. Here the steady-state result can be thought of as an approximation to the peak value (of burning rate or rate of heat release) seen experimentally. The approximation is rough but the simple model is instructive nonetheless.

For Case (1), burning on one side only, the steady-state heat balance becomes the following:

$$q_{\text{ext}} + \zeta h (T_f - T_s) = Q_s l_s Z_s \exp(-E/RT_s) + \sigma (T_s^4 - T_0^4) \dots\dots(1)$$

Here q_{ext} is the external radiant flux; the material is assumed to have a negligible reflectivity for this flux. The second term in Eq (1) is the convective heat feedback from the flame whose temperature is T_f (taken to be independent of incident heat flux); h is the convective heat transfer coefficient between flame and sample surface and the quantity ζ is a correction to this for blowing of the flame in the buoyant boundary layer. This is dependent on the mass flux from the surface and is computed from an expression derived by Spalding [5]:

$$\zeta = (m C_g/h) / (\exp(mC_g/h) - 1) \dots\dots\dots(2)$$

Here m is the mass flux from the surface (one half of the total gasification rate throughout the sample depth) and C_g is the heat capacity of the gas. The value of ζ varies from zero for an infinite gasification rate to one for no gasification. The two heat sources on the left in Eq (1) are balanced by the two heat sinks on the right. The first term on the right is the heat required to gasify the solid fuel; Q_s is the heat of gasification (endothermic), l_s is the sample thickness, Z_s and E are kinetic parameters of the gasification process, R is the gas constant, T_s is the sample temperature. This first term on the right, with the reaction heat Q_s omitted, is the total volumetric gasification rate (twice the value of m in Eq(2)). The last term in Eq (1) is the net radiative loss from the front surface of the sample; σ is the Stefan-Boltzmann constant and T_0 is the ambient temperature. The rear surface of the sample is assumed to be adiabatic.

For case (2), both surfaces irradiated and burning, the steady-state heat balance is very similar.

$$2 q_{\text{ext}} + 2 \zeta h (T_f - T_s) = Q_s l_s Z_s \exp(-E/RT_s) + 2 \sigma (T_s^4 - T_0^4) \dots\dots(3)$$

All of the symbols have the same meaning as in the previous case.

Equations (1) and (3) are transcendental algebraic equations which define the steady-state value of T_s , the sample temperature; this in turn defines the rate of gasification of the sample and its heat release rate (gasification rate times heat of combustion of the gases). Clearly the two physical situations will not lead to the same value for T_s ; this temperature will be higher for case (2) above because of the doubling of the heat source terms. The tendency for T_s to increase as a result of this heat source doubling is damped by the increased radiative loss (also doubled) and the tendency for the parameter ζ to decrease when the mass flux from the surface tries to increase (the flame is blown further out from the surface and thus heats it less effectively).

The equations for these two cases have been solved by a Newton-Raphson iteration technique to find T_s . The parameters have been chosen to be similar to those in the experiments described below, but are not identical, particularly since the gasification kinetics of the materials used there have not been determined. The values of the convective heat transfer coefficient and the flame temperature were chosen so as to put the flame heat feedback flux in the right neighborhood (approximately 30 kW/m²). The kinetic parameters were chosen so that the overall gasification rate is comparable to that measured experimentally. The gasification heat used was a rather generic value (200 cal/g or 840 J/g). To compute a rate of heat release from the gasification rate, a heat of

combustion comparable to that seen experimentally was used (20 kJ/g).

Since this tendency for the sample temperature to vary with heat input rate is a consequence of the Arrhenius temperature dependence of the gasification rate, the activation energy, E , was varied to assess its impact. When this was done, the value of Z_s was adjusted so as to keep the gasification rate at 400 C a constant value; otherwise a very artificial sensitivity would have been seen. This temperature, though somewhat arbitrary, is close to what one expects for the materials studied here.

At this point it is necessary to point out one of the complications that the experimental apparatus introduces. The apparatus (described in detail below) cannot separate gases evolved from the front or from the back of the sample and gases can freely evolve from both sides. The vertically-oriented sample sits on a weight cell so that the total weight loss rate is seen. Furthermore, the gases which come from the back of the sample during one-sided heating inevitably burn when they meet the front face flame at the top of the sample (this top flame does not feed heat back to the rear surface of the sample). Thus the rate of weight loss and heat release seen in the one-sided case are double the value that the model above (Eq. (1)) implies. Because the model results are later to be compared with experimental results, the model results were expressed on the same basis, i.e., the rate of heat release reported here for case (1) is twice the value one would get if the premises of the model were strictly adhered to.

Figure 1 shows the result of solving the two cases and calculating the rate of heat release in the manner just indicated. The incident radiant flux has been varied over a range comparable to that used experimentally. One sees that the behavior is not greatly sensitive to the value of the activation energy, E . The two-sided heating/burning case is predicted by this steady-state model to yield somewhat less than a factor of two increase in rate of heat release for the conditions of the experiments described below. If the gases from the rear of the sample did not burn, the one-sided rates of heat release would be half the values shown by the solid lines; the dashed line shows where they would fall. The predicted ratio of heat release rate between the two cases would then be greater than three. Recall that the thermally-thick case would yield only a factor of two.

Transient model. The most unrealistic physical element of the preceding model is the neglect of solid fuel consumption. It contains those essential features of the real problem necessary to demonstrate the origin of the burning rate enhancement when a thermally-thin material is burning on both sides. However, the real problem is inherently transient because fuel is being consumed even as the sample proceeds from ignition toward a peak burning rate condition; this affects the value of that peak. Thus the

preceding model is missing features which could affect the quantitative prediction of the ratio between one and two-side burning rates.

The only new elements in the transient model are the changing heat content of the solid fuel and its changing mass. To deal with these requires the simultaneous solution of two, coupled ordinary differential equations which express the conservation of energy and solid fuel mass. Most of the terms in the energy balance are again the same. Both the one and two-sided heating/burning cases can be expressed by the single set of equations below.

$$(\rho_s C_s l_s) dT_s/dt = f (q_{ext} + \zeta h(T_f - T_s) - \sigma(T_s^4 - T_0^4)) \\ - Q_s l_s Z_s (\rho_s - \rho_{res}) \exp(-E/RT_s) \dots\dots\dots(4)$$

$$d\rho_s/dt = -Z_s (\rho_s - \rho_{res}) \exp(-E/RT_s) \dots\dots\dots(5)$$

The first term in Eq.(4) is the transient heat content of the solid fuel. The terms on the right hand side of this equation are essentially the same as in the steady-state models. The quantity ζ is given by Eq. (2) as before. The factor f is one for the one-sided heating/burning case and two for the two-sided case. The fuel concentration in the solid now is expressed explicitly in the fuel gasification rate term; it was implicit in Z_s in the steady-state models since it was not a variable as it is here. The quantity ρ_{res} is the residual mass of the sample after all of the fuel is consumed. This has been introduced because all of the experimental samples are composite materials with a substantial glass fiber content. Equation (5) expresses the conservation of solid fuel mass.

In order to implement this model a statement has to be made about when the flame appears (flaming ignition). A complete description of the runaway to flaming in the gas phase would require a much more complex model. Instead, use is made of the idea that there is a critical fuel mass flux level at which the flame appears [6]; in the experiments there is a spark igniter which ignites the gases as soon as they reach a flammable concentration. This simplification should be quite adequate for this model.

The equations are solved by an explicit time-marching method (Runge-Kutta 4) starting from the first appearance of the flame. Since the mass flux at this point is prescribed (2.5 g/m² sec, from Ref. 6), the temperature and initial density can be determined, as well, assuming negligible reactant consumption prior to ignition. The model could be used to predict the time it takes the external radiant flux to raise the sample to this "ignition temperature" but

that is tangential to the main objective here. Time steps of 1/16 second give energy and mass balance errors no greater than a few tenths of a percent. When fuel consumption is artificially suppressed this program converges to the same steady-state solutions as does the steady-state model above.

Figures 2, 3, and 4 show the output of a typical case predicted by the transient model. The parameters not shown explicitly are the same as those used in the steady-state model predictions. Figure 2 shows that the temperature of the sample climbs continually from the moment of ignition while Fig. 3 shows that the fuel mass decays monotonically; the result, in Fig. 4 is a rate of heat release that goes through a peak about midway through the burning process. Burning is terminated in the model when the mass flux from the surface again drops to the critical level for flaming. Figure 5 shows that the time that the heat release rate peak is reached is sensitive to the activation energy of the gasification process; the height of the peak is weakly sensitive to this parameter.

Figure 6 shows a set of results from the transient model that is comparable to the steady-state set in Fig. 1. The more realistic transient model predicts lower peak rates of heat release. It also indicates a factor somewhat less than two between the rates of heat release from the one and two-sided cases. Recall that the one-sided results as shown here assume the gases from both sides contribute to the reported rate of heat release; the dashed line shows where the one-sided results would fall if the gases from the back of the sample did not contribute to the rate of heat release. Comparison of the position of the dashed line with the two-sided results shows that there is still a factor greater than three between the one and two-sided heating/burning cases. A comparison of these predictions with experimental measurements is made below.

Experimental Details

The NIST Cone Calorimeter is a device which measures rate of heat release from a burning object using oxygen-consumption calorimetry. The plume of products from the burning object is captured completely. Its flow rate and oxygen content are monitored continuously (5 second intervals). From these data and the fact that nearly all organic compounds evolve essentially the same amount of heat per gram of oxygen consumed, one can infer the rate of heat release to an accuracy of about $\pm 5\%$.

This device was designed to irradiate and measure samples burning on one side only. To use it for the present work it was necessary to remove the cone-shaped heating element and design a new device that could irradiate both sides of a thin, vertically-oriented sample simultaneously (and equally). The device that was built for this purpose is shown schematically in Fig. 7. It consists of a matched pair of planar heater assemblies, each 17.8 cm square,

oriented vertically in a suitable holder with a gap of 3.2 cm. The heat source within each heater assembly is a 2500 watt heater cable shaped into a zig-zag pattern. Nickel elements placed between each rung of this pattern serve to spread the heat by conduction and pass it to nickel sheets (17.8 cm square) which form the face of each heater assembly. Each heater assembly is run by a constant temperature controller. The heat flux from each face can be measured by a Schmidt-Boelter gage placed at the same position as the center of the sample face. The system was designed to impose a uniform heat flux on a sample whose exposed face is 7.6 cm square. Actual measurements show the deviations above the horizontal centerline of the sample were about 3%; below the centerline they were 5%. The dynamics of the heater control were such that some upward drift in heater temperature (5 -10 C) occurred during sample exposure; this yields a change in the incident heat flux of less than 5%.

The samples, all 0.16 cm thick, were 8.25 cm square. The 0.125 cm peripheral edge surrounding the exposed face was loosely held between a minimal framework cut from 0.051 cm thick stainless steel sheet to reduce heat sinking on the sample edges.

All three of the samples tested were composite materials; see Table 1. Previous experience with composites has shown that they have a distinct tendency to develop internal bubbles during intense thermal degradation which then can lead to erratic jets of gases emerging at unpredictable times and locations. To eliminate this tendency, all samples had a pattern of very small holes drilled through them (0.13 cm dia.). Preliminary experiments established that a hole spacing of 0.6 cm yielded only weak gas jets which tended to merge into an essentially continuous flame sheet on the face(s) of the sample. This precluded practically all contact of the sample flames with the radiant heaters.

The vertical orientation of the samples (necessary to yield equal flames on the two faces) yielded a buoyant boundary layer which preferentially cooled the lowest portion of the sample face, countering the radiant heating somewhat. This is a two-dimensional effect not included in the models above. As a consequence of this slightly lesser net heating rate for the lower portion of the sample, ignition tended to occur first on the upper 1/2 to 2/3 of the irradiated face(s). The flame then spread down to envelop the entire face. When the rate of heat release per unit area is computed from the raw experimental data, it is normally assumed that the full face is burning from ignition onward. The focus here is primarily on the peak burning condition (peak rate of heat release). Most of the tests were video-taped so that the extent of sample face burning could be determined as a function of time. In some cases, the full face was not burning when the peak heat release rate was reached. The worst case was about 90% area involvement at the time the peak occurred; the peak values reported here have been corrected for this effect when the tapes showed it

was present. This correction, which is for the actual burning area only, cannot fully eliminate the effects of non-simultaneous ignition of the full sample face. The peak is also lowered somewhat by the fact that the area which first ignited has undergone some fuel depletion by the time lower portion of the sample face is fully ignited.

Recall that the model assumes that the one-sided burning case is adiabatic on the non-irradiated face. Also, half of the gases generated within the sample are assumed to emerge from that face. To approximate this condition as closely as possible, the unexposed face of the sample was insulated with 0.6 cm of ceramic fiber insulation placed on the outside of an aluminum foil wrap. The foil was wrapped on the edges of the sample but, on the unexposed face, there was a gap of $1\frac{1}{2}$ to 2 mm which opened to the top of the sample face only. This arrangement approximated the adiabatic back surface condition while allowing gases from the rear face to pass freely to a location where their burning would not feed heat to the sample. In the two-sided burning cases, only the sample edge was wrapped with foil to inhibit any tendency for gases to evolve there.

Experimental Results

Figure 8 shows a typical rate of heat release curve, annotated so as to indicate the various stages of burning of the sample. The sample ignites at 166 seconds after the start of the irradiation, in this case, on one face only. There is essentially immediate involvement of the upper half of the irradiated face but it takes another 17 seconds for the flame to spread over the full face. Here this full spread is complete well ahead of the peak in the rate of heat release curve. This spread tended to be somewhat slower for the other two materials, but, as noted above, spread was nearly always complete before the peak was reached. On the other side of the heat release peak, the video tapes consistently showed that the central region of the sample extinguished first. The spread between "center dying" and "edges only" indicates some ambiguity in the timing of this. The first notation indicates the earliest hint that the flames in the center of the sample face were weakening; the second notation indicates the time at which only the periphery of the sample continued to flame.

In addition to these non-one-dimensional effects on the beginning and end of the experimental heat release rate curves, there is some distortion (flattening) of the peak due to instrument characteristics. Both flow dispersion in the gas sampling lines of the Cone Calorimeter and the finite response time of the oxygen analyzer (7-8 sec for 90% response to a step change) contribute to an overall system response time of about 10-12 seconds for 90% response to a step change. This is not a significant problem with data such as that in Fig. 8. It is significant (but not large) for the shortest

tests (highest flux on two faces of the sample) where the bulk of the heat release peak is only about 30 seconds long. The underestimate of the true peak height should be less than 10% in these worst cases.

At this point, with the time scales in Fig. 8 in mind, it is pertinent to examine the extent to which the samples behave in a thermally-thin manner. Recall that in the ideal case this implies no temperature gradient at all in the depth of the sample. Carslaw and Jaeger [7] present solutions to a relevant heat conduction problem, that of an inert, slab-like sample heated by a constant flux on one face with the other face being adiabatic. As such a sample heats up, it retains a front to back temperature difference relative to the increasing average temperature. That fractional difference, divided by the mean temperature, is given by the following expression.

$$\text{Fraction} = 0.5 l_s^2 / (\alpha t) \quad \dots\dots\dots (6)$$

Here l_s is the sample thickness, as before; α is the thermal diffusivity of the sample and t is the time over which the sample has been subjected to the constant front surface heat flux. Note that this fraction decreases with time. Using a value for α of $0.0019 \text{ cm}^2/\text{sec}$ derived from data in Ref. 8 and the 0.16 cm thickness of the samples used here, one finds

$$\text{Fraction} = 6.7/t \quad \dots\dots\dots (7)$$

At the low end of the flux range used here (ca. 20 kW/m^2) the ignition time for one-sided irradiance was of the order of 200 seconds. At the high end of the flux range (ca. 40 kW/m^2) it was as short as 70 seconds. Assuming ignition occurs at $300\text{--}350 \text{ C}$, one finds front-to-back temperature differences at ignition time which are a small fraction of the mean temperature. However, particularly at high fluxes, the inferred differences (ca. 30 C) are not small in terms of their potential effect on the sample degradation/gasification process. The Arrhenius temperature dependence of the chemical reactions serves as a large amplifier of this relatively small temperature difference. Fortunately the endothermicity of the reactions tends to damp this temperature difference. That is, as soon as the front-to-back temperature difference starts to cause the front to gasify preferentially, the heat absorbed by this reaction slows the local rate of temperature rise and helps bring the front and back of the sample more into temperature equality. The quantitative extent to which this forces a more constant temperature through the sample depth can only be assessed in the context of a thermally-thick model. The thermally-thin model above shows that the chemical heat sink term is comparable to

the thermal capacitance term so the potential for temperature smoothing is there. The holes through the samples, described above, also should help push toward the idealized behavior of equal mass fluxes from the front and back of the sample. In any event, it is clear that the ideal extreme of thermally-thin behavior is approached here but is probably not achieved.

The measured data on each of the materials comprises complete rate of heat release curves at three (or more) flux levels. For present purposes it is sufficient to examine only the behavior of the peak rate of heat release, as was done with the model results in Fig. 6. Figures 9, 10 and 11 show such results for the three materials described in Table 1. All are plotted on the same scale though it should be noted that the scales in the plot of the model predictions (Fig. 6) are different. Examination of these Figures shows that there is a distinct tendency for the ratio of two-sided to one-sided peak heat release rate to be greater than is predicted by the transient model. The ratio in Figures 9-11 is greater than two whereas in Fig. 6 it is less than two. When one recalls that the one-sided peaks should be divided by a factor of two to eliminate the heat release from the gases evolved from the rear surface, the stronger synergistic effect in the two-sided experimental results is even more striking. The ratio of the two-sided to one-sided peaks is then 4 to 5, as compared to a factor of two expected for thermally-thick materials.

The reasons why the experimentally observed synergism is greater than that predicted are not completely clear. It must be borne in mind that the model cannot be expected to be quantitatively accurate since the kinetic parameters it uses have not been measured. In addition, the description of the effects of boundary layer blowing (Eq. (2)) on the flame heat feedback is qualitative at best for these samples with their pattern of holes. The non-ideal effects in the experiments discussed above should have mixed effects. The finite instrument response time will lower the two-sided heat release peaks more than the one-sided peaks but, as indicated above, this effect is probably not appreciable here. The impact of a departure from true thermally-thin behavior is harder to judge but its main effect is probably to cause a somewhat greater flow of gasification products out the front face of the sample (versus the back) in the one-sided heating case. Then the one-sided peaks should be divided by a factor somewhat less than two in inferring the ultimate degree of synergism in the above discussion. Another secondary factor with a similar effect is variation in flame temperature; recall that it was taken to be constant in the models. The back surface in the one-sided burning case will be less than perfectly adiabatic (though the insulation scheme used should be quite effective); this will somewhat lower the flame temperature. This loss is absent in the two-sided burning case which also has more net energy input via the incoming radiation on the second surface; thus the flame temperature should be relatively higher.

Implications for Material Flammability

The first implication of the synergism is already clear; when a thermally-thin material burns it gives off heat at a substantially greater rate than one might expect on the basis of a one-sided burning test. Clearly it must do so for a proportionately lesser time, however. (The total energy evolved will not be affected but, since the heat release is a non-constant transient, the reduction in burn time will not necessarily be by the same factor as the change in peak heat release rate.)

The change in peak heat release rate brings with it the possibility that the tendency for flames to spread over the material will be altered. One and two-sided opposed flow flame spread have not been examined in this study but this process is dominated by solid and gas phase heat conduction at the leading edge of the flame. It is not clear that the synergistically-enhanced mass flux that would result in the two-sided case would result in an equal (or any) synergism in flame spread rate beyond the factor of two normally expected.

To make an assessment of the possible enhancement of concurrent flame spread, the model of Cleary and Quintiere [9] is useful. That model, which is qualitatively applicable to the small scale, laminar flame conditions of the NASA flammability test, leads to an expression for the critical heat release rate necessary for concurrent flame spread.

$$Q^* = (1 / k_f) ((t_{\text{ign}} / t_b) + 1) \dots\dots\dots(8)$$

Here Q^* is the minimum rate of heat release on the ignited portion of a material for concurrent spread to proceed indefinitely in the direction of gas flow over the material. The quantity k_f is a proportionality factor between heat release rate and flame length in the direction of spread; t_{ign} is the ignition delay time of the material at the flame heat flux; t_b is the burning time of the material once it is ignited.

Compare the one-sided and two-sided heating/burning cases in the context of this criterion for concurrent flame spread. To a first approximation the proportionality constant k_f is the same for both cases. (There are some complications here due to applying a turbulent flame model to the laminar situation that exists in small scale flammability test; see Ref. 1.) The ignition delay time at the flame heat flux will differ by a factor of two between the two cases; the two-sided spread case will ignite in half the time since the mass being heated by each flame is halved. The burn time also tends to change by about a factor of two. In the experiments

described above, the total burn time in the two-sided cases decreased by very nearly a factor of two in the low flux cases but the decrease was closer to a factor of three at the high end of the incident flux range. The ratio (t_{ign}/t_b) in Eq. (8) is in the range from about 1.5 (high incident flux) to 5 (low incident flux) for the materials tested here so the high flux changes in t_b (beyond a simple factor of two) influence Q^* rather weakly. From the preceding one infers that, for the low incident flux cases, Q^* is unchanged; for the high incident flux cases, it increases less than 50%. Combining this with the strong increases in rate of heat release seen in the two-side cases above, one infers that the two-sided case is always more prone to concurrent flame spread than is the one-sided heating/burning case since it is more likely to exceed the above criterion for spread.

There is one further subtlety that is pertinent to such testing. When a fixed ignition source, such as the NASA 8060.1C chemical ignition source, is used to test a material in a one-sided versus a two-sided exposure, the latter is in one sense less severe. Splitting the igniter flame between the two surfaces halves the effective rate of heat release and thus reduces the igniter flame length on the two sides of the sample [6]. The igniter's rate of heat release helps drive the initial flame spread process up the face of a sample and can have a substantial impact on whether the flame spreads beyond a fixed pass/fail length. A completely equitable comparison of one-sided and two-sided ignition and concurrent flame spread hazards would call for two igniters in the two-sided case, one on each side of the sample. Of course it can be argued that this is a highly improbable occurrence in actual practice.

This study clearly demonstrates that two-sided burning of thermal-thin materials is, for the synergistic reasons which emerge from the models above, more hazardous than one-sided burning. Thus it is clearly important to test thin materials in this manner in keeping with the idea of a worst case assessment of their potential hazard.

Chapter Three

Design of an Experiment to Demonstrate the Effects of Self-Feedback of Radiation on Flamespread Behavior

Introduction

An important point illustrated by the results of earlier studies in this program [1], and by numerous other material flammability studies, is that external radiation impinging on a material before and during its burning can have a major impact on its flammability behavior. Such radiation shortens ignition delay times, increases the rate of heat release from a material once ignited and increases the rate at which flames spread over the surface of the material.

This radiation could be coming from a nearby hot or burning object. The close control which NASA exercises over material placement in spacecraft so as to preclude paths for fire spread should lessen (not necessarily eliminate) such sources of radiation. However, another source of such radiation is the burning object itself. The object may have a concave surface whose shape presents finite radiative view factors between burning surface elements. Then such elements will exchange radiation and enhance each others flammability. The enhancement occurs because the radiative exchange partially (or even totally) cancels the radiative loss from the burning surface which normally plays a substantial role in lessening material flammability.

Such radiative feedback (or self-feedback) is expected to be largely dictated by the surface temperature of the burning material. For some materials this should substantially limit the flux levels to be achieved. For example, many pure thermoplastics can be expected to have a burning surface temperature in the range of 350-450 C; a blackbody at 450 C emits 15 kW/m². The flame zone, if very sooty, might supplement this somewhat. However, the flame can play a more complex role in materials that either char or contain inert fillers or reinforcements. Such residual materials tend to form a layer on the burning (or burned) surface; if the flames make contact with this surface layer it can be heated to temperatures well beyond the levels just noted. The radiation from the surface will rise strongly with temperature. Thus it is difficult to predict a priori what levels of radiation are pertinent to self-feedback processes.

In view of the potential importance of the self-feedback of radiation and the uncertainties in its magnitude, there is a strong need to examine this issue experimentally. An experiment of this nature is described below. Its goal is to vary the self-feedback of radiation to a burning surface, quantify the radiation level and demonstrate its effect on flame spread processes. The effect

should be found to be comparable to imposing the same flux levels with an external source of radiation.

Experiment Design

Perhaps the simplest sample geometry for this purpose is two parallel flat surfaces oriented vertically. Two flat surfaces provide a geometry that facilitates ready estimation of the radiative view factor over the burning surface; the vertical orientation provides well-defined buoyant flow. The situation bears a substantial resemblance to that discussed in Chapter 2; the radiative self-feedback plays the same role as the external radiation in Equations 1 and 3 of that Chapter.

The radiative feedback is to be varied by changing the burning area on the sample face. Producing controlled changes in this burning area is actually one of the biggest challenges of doing this experiment. Rather than try to do this equally for two parallel surfaces, the second burning surface is replaced by a flat mirror which creates an identical image of the one surface that is actually burning. Except for a slight loss due to mirror absorption, this yields the same feedback flux as would a second burning surface. However, the mirror must be at half the distance from the actual burning surface that a real second surface would be.

Figure 12 shows the calculated view factor along a line normal to the center of a square radiating area. Along this line the value of the view factor depends only on the ratio of the width of the square to the distance that the receiving point is from the center of the square (gap width between the burning surface and its image in the mirror). When this ratio is ten the view factor is nearly at its maximum value of unity. By fixing the gap width at 3 cm and varying the width of the burning area on the fuel surface (in successive experiments) from 4½ to 24 cm., one can vary the radiative view factor from 0.4 to 0.95. Figure 13 shows that the feedback flux that will result will not be uniform over the burning area since the view factor inevitably falls off as one approaches the edge of the burn area. This is inherent in the nature of self-feedback and so must be viewed as a complicating but necessary aspect of the experiment. It implies that the level of flammability enhancement caused by a given peak self-feedback flux level may not be identical to that caused by an equal, but spatially-uniform external flux. The two effects should be proportional but the self-feedback enhancement should be less if measured by its peak flux level.

It would be most desirable to apply this type of self-feedback demonstration in the context of upward or concurrent flame spread. Upward spread is used in the standard NASA flammability screening test. Concurrent flame spread, in general, is expected to be a

greater hazard than is opposed-flow flame spread because it is inherently more efficient in heating the next element of fuel toward which the flame is moving. However, such flame spread is sensitive to the ignition process (igniter heat release rate per unit width) in addition to intrinsic material properties. It is more difficult to demonstrate radiative feedback effects in concurrent spread because the varied igniter area, mentioned above, simultaneously affects two factors governing the viability of upward spread. There may be ways to overcome this but the experiment described here avoids this complication by focusing instead on opposed flow flame spread; this spread mode has no dependence on igniter heat release rate.

The opposed flow flame spread processes in the current experiment are lateral and downward spread on a vertical surface. The goal is a quantitative demonstration of the ability of self-feedback to enhance this form of spread. For many (perhaps most) materials burning on a single surface, once the ignition source is removed, cannot be sustained because of excessive heat losses. Thus the first form of enhancement to be seen from self-feedback is stabilization of the burning process on the ignited area. The next form, presumably requiring a higher level of feedback, is lateral spread, then downward spread. Both will occur at increasing velocities as the feedback flux increases. This is the qualitative sequence seen with external radiation and it should carry over to self-feedback.

The essential components of the experimental apparatus are sketched in Fig. 14. The vertically-oriented sample is a flat rectangle which can be up to 25 cm wide and 35 cm tall. The front surface mirror and multiple gas jet igniter are essentially the same dimensions. The igniter face has an extensive array of holes (1765 on 6 mm centers) to which are attached small pre-mixed flamelets pointing upward at a 45 degree angle; this angle eliminates the sharp, highly localized convective heat transfer from stagnation points that would exist with normal jet impingement. The actual igniter area that is used is varied from a $4\frac{1}{2}$ cm square to a 18.3 cm square; the full 25 cm width can be used as well. For a 3 cm effective gap width ($1\frac{1}{2}$ cm between sample surface and the mirror) the smallest ignited area gives a radiative view factor of about 0.4; the largest gives a view factor of nearly one. The view factor can be reduced further by increasing the gap width.

The mirror is aluminized on its front surface and has a silicon monoxide overcoat. The reflectivity in the infrared (beyond 2 μ m) for this coating combination is typically greater than 95%. The substrate is Pyrex which will allow heating of the mirror from the back to prevent condensation. The gap between sample surface and mirror will have to be sufficient to preclude flame impingement and/or soot deposition.

It is necessary to be able to shift quickly between having the ignition position and the burning position. This is facilitated by combining the mirror and igniter into a single assembly which can be moved laterally on a rail. During ignition the igniter is shifted to the left (Fig. 14) and the sample is moved forward so as to make contact with the flamelets; the high flux assures rapid ignition with a minimum of sample consumption. When ignition is achieved, the sample is moved back to give the desired gap width and the mirror/igniter assembly is moved to the right, putting the mirror in front of the sample. The subsequent behavior of the burning zone on the sample face is followed via two video cameras, one looking from above and the other looking from one side.

All of the essential parts of this apparatus have been constructed but not yet assembled. Before this a small version of this set-up was constructed and tested to assure the feasibility of the experiment. This did point out some complications in the achievement of the desired uniform ignition conditions with the igniter; a fix was devised which did achieve this. It should work similarly for the full scale apparatus.

Data for two composite materials were obtained in our modified version of the NASA flammability assessment apparatus for the effect of external radiation on opposed-flow flame spread. Partial data were obtained for a third material. In this experiment, the results of which are to be compared with those from the above apparatus, the NASA igniter impinges on one region of the sample face. The external radiative flux is varied (in successive experiments) to find the quantitative impact it has on flame stabilization and lateral/downward spread velocities. These data will be reported when the above experiments are completed.

Chapter 4

Conclusions and Recommendations from this Study

- 1) In a comparison done in atmospheric oxygen, several materials which passed the standard NASA flammability screening test for resistance to upward flame spread exhibited widely varying degrees of flammability as measured in ignitability, rate of heat release and opposed flow flame spread tests developed at NIST.
- 2) In view of the above result, materials which pass the standard NASA flammability screening test should not be considered to be non-flammable. The NIST tests show that the tested materials, like most other organic materials, burn when subjected to external radiation. The sensitivity to external radiation is highly variable and may not be evident from the result of a standard NASA screening test.
- 3) The behavior of these same materials as seen in the NIST tests cannot presently be quantitatively correlated with the NASA test behavior.
- 4) It is desirable to supplement the results of the standard NASA screening test with a modified version which incorporates external radiation. Such supplementary testing is particularly needed for materials which are used (or contemplated for use) extensively in manned spacecraft interiors. A flux of 20 kW/m^2 is tentatively suggested until further information on real fluxes is available. The self-feedback experiment described in Chapter 3 of this report can provide the real data on the fluxes to be seen in actual fires.
- 5) There is a pressing need to establish a greater understanding of the relation between flammability in normal gravity and micro-gravity. Since this is a considerable, longterm undertaking and the need is immediate, a pragmatic nearterm approach is indicated. This could consist of an experimental program to establish a correlation, for a limited series of realistic materials, between the modified NASA test suggested above and the micro-gravity flame spread behavior of these same materials as a function of both external heat flux and ambient gas flow velocity. This would necessitate the development and use of an experimental package that could be flown aboard a sounding rocket. Without such information, spacecraft designers are confronted with unquantifiable risks regarding fire safety.
- 6) The results of Chapter 2 in this report confirm that, for thermally-thin materials, two-sided burning is substantially more hazardous (in normal gravity and probably also in micro-gravity) than is one-sided burning. The current NASA test incorporates this

effect by virtue of its symmetrical igniter placement for thin materials.

Acknowledgements

K. Villa and R. Shields provided extensive assistance in the various experimental aspects of this program.

References

- 1) Ohlemiller, T. and Villa, K., "Material Flammability Test Assessment for Space Station Freedom", National Institute of Standards and Technology NISTIR 4591, June, 1991 (also NASA CR-187115)
- 2) Kimzey, J., "Skylab Experiment M-479, Zero Gravity Flammability", Johnson Space Center Report JSC 22293, August, 1986
- 3) Olson, S., Ferkul, P. and T'ien, J., Proceedings of the Twenty-Second Symposium (International) on Combustion, The Combustion Institute, Pittsburgh (1988), p.1213
- 4) Steinberg, T. in "Findings of a Review of Spacecraft Fire Safety Needs", Apostolakis, G. et al, UCLA Mechanical, Aerospace and Nuclear Engineering Dept. Report UCLA ENG 92-19, March, 1992
- 5) Spalding, B., Int. J. Heat and Mass Transfer, 1, 1960, p.192
- 6) Parker, W., "Prediction of the Heat Release Rate of Wood", Ph. D. Thesis, Dept. of Mechanical Engineering, George Washington University, Washington, D. C., April, 1988
- 7) Carslaw, H. and Jaeger, J., Conduction of Heat in Solids, Second Edition, Oxford at Clarendon Press, 1959, p. 112
- 8) ASM International, Engineered Materials Handbook, Vol. 1, Composites, ASM International, Metals Park, Ohio, 1987, p. 405
- 9) Cleary, T. and Quintiere, J., "A Framework for Utilizing Fire Property Tests", in Fire Safety Science-Proceedings of the Third International Symposium, Elsevier Applied Science, New York, 1991, p.647

Table 1

Description of Test Materials
in One vs Two-Sided Burning Study

<u>Material</u>	<u>Thickness (cm)</u>	<u>Description</u>
Haysite ETS****	0.16	A thermoset polyester reinforced with swirl mat glass fiber; organic resin content 37% by weight; 160 C mechanical rating.
Haysite H755	0.16	Polyester resin reinforced with swirl mat glass fiber; organic resin content 38% by weight; 165 C mechanical rating.
Epoxy/glass circuit board	0.16	G-11 NEMA rating (unretarded); woven roving glass; organic resin content 32% by weight; 177 C operating temperature rating.

****Haysite Reinforced Plastics, Inc., Erie, Pennsylvania 16509

FIGURE 1
STEADY-STATE MODEL RESULT
ONE AND TWO-SIDED HEATING/BURNING

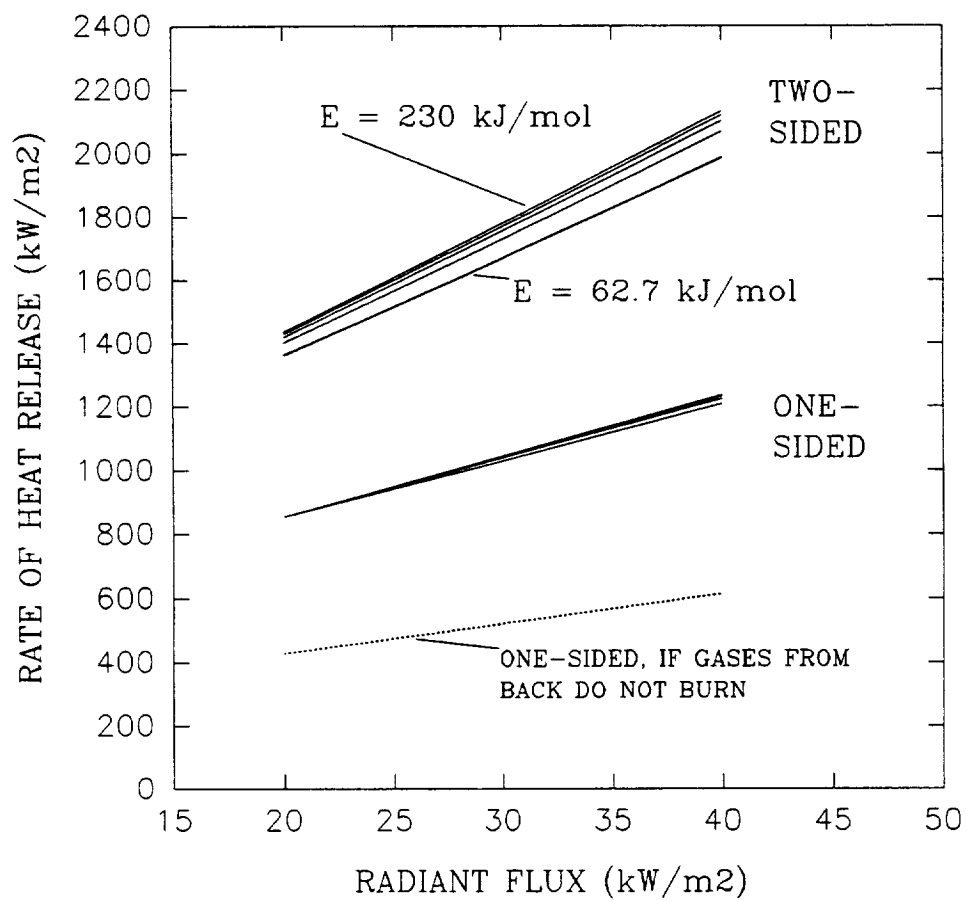


FIGURE 2
TRANSIENT MODEL RESULT
ONE-SIDED HEATING/BURNING

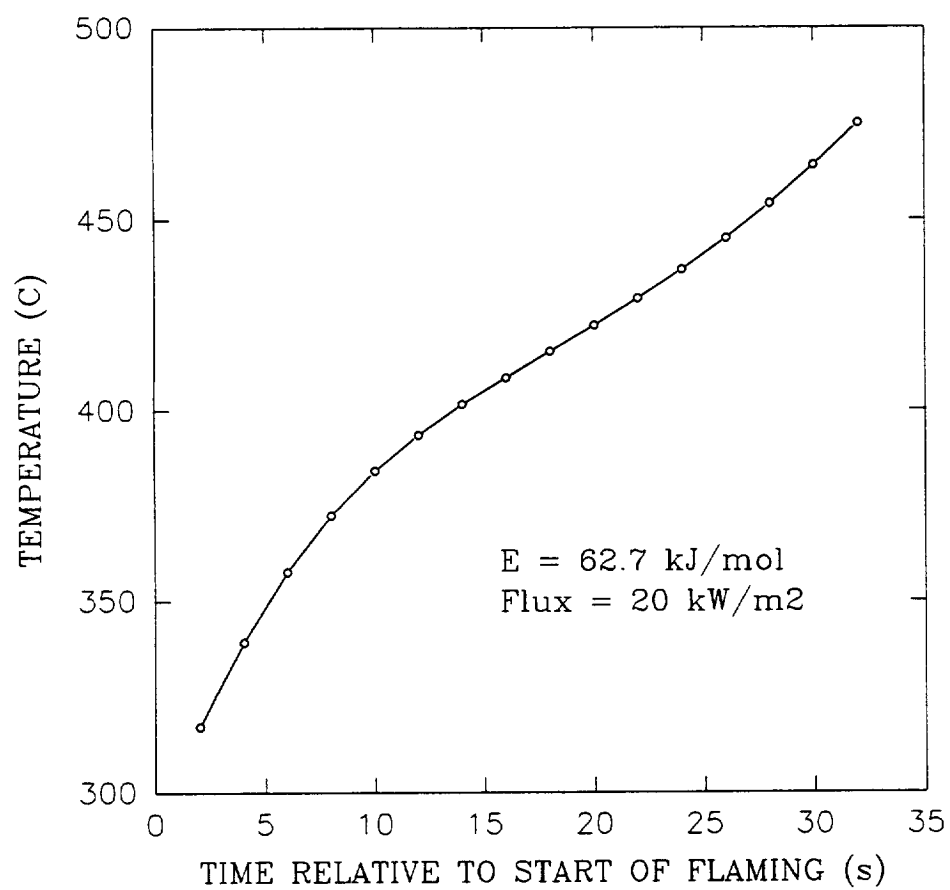


FIGURE 3

TRANSIENT MODEL RESULT

ONE-SIDED HEATING/BURNING

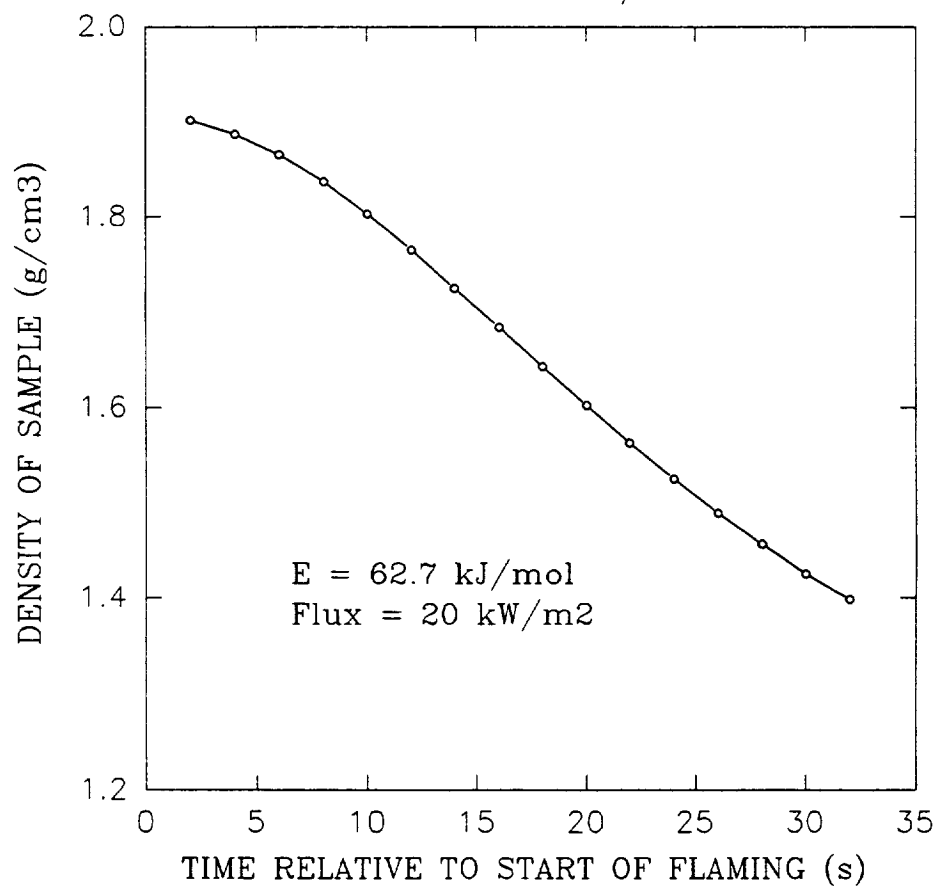


FIGURE 4
TRANSIENT MODEL RESULT
ONE-SIDED HEATING/BURNING

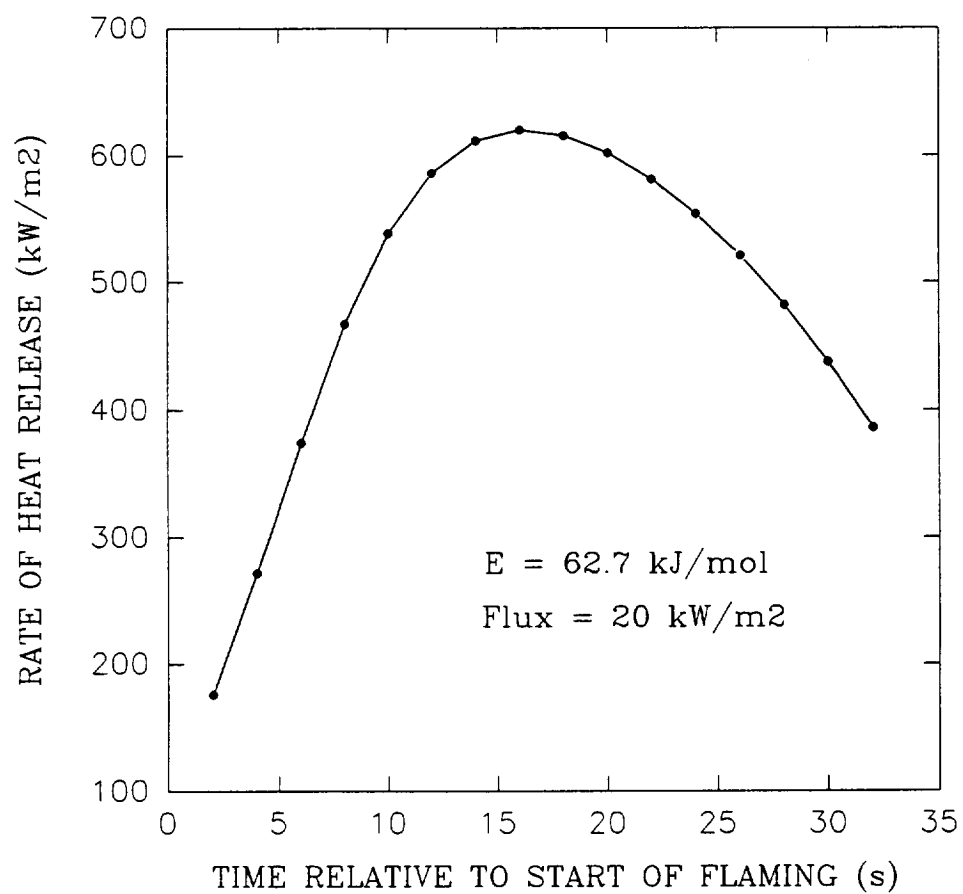


FIGURE 5
TRANSIENT MODEL RESULT
EFFECT OF ACTIVATION ENERGY ON RATE OF HEAT RELEASE

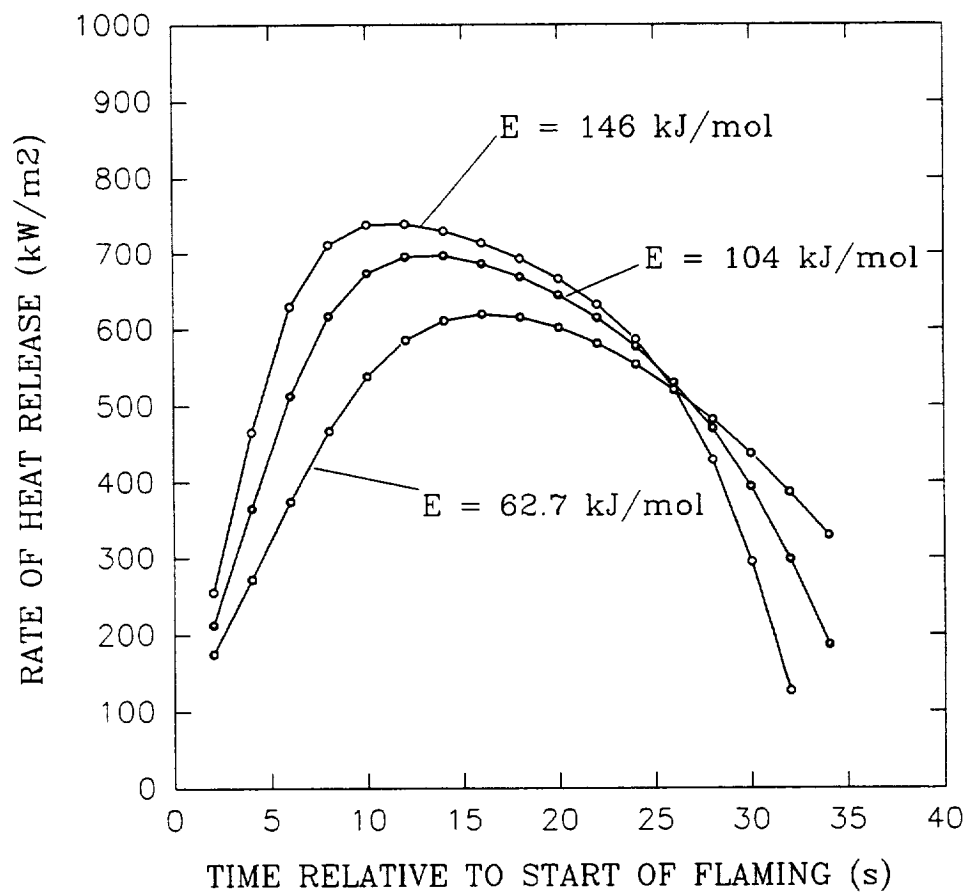
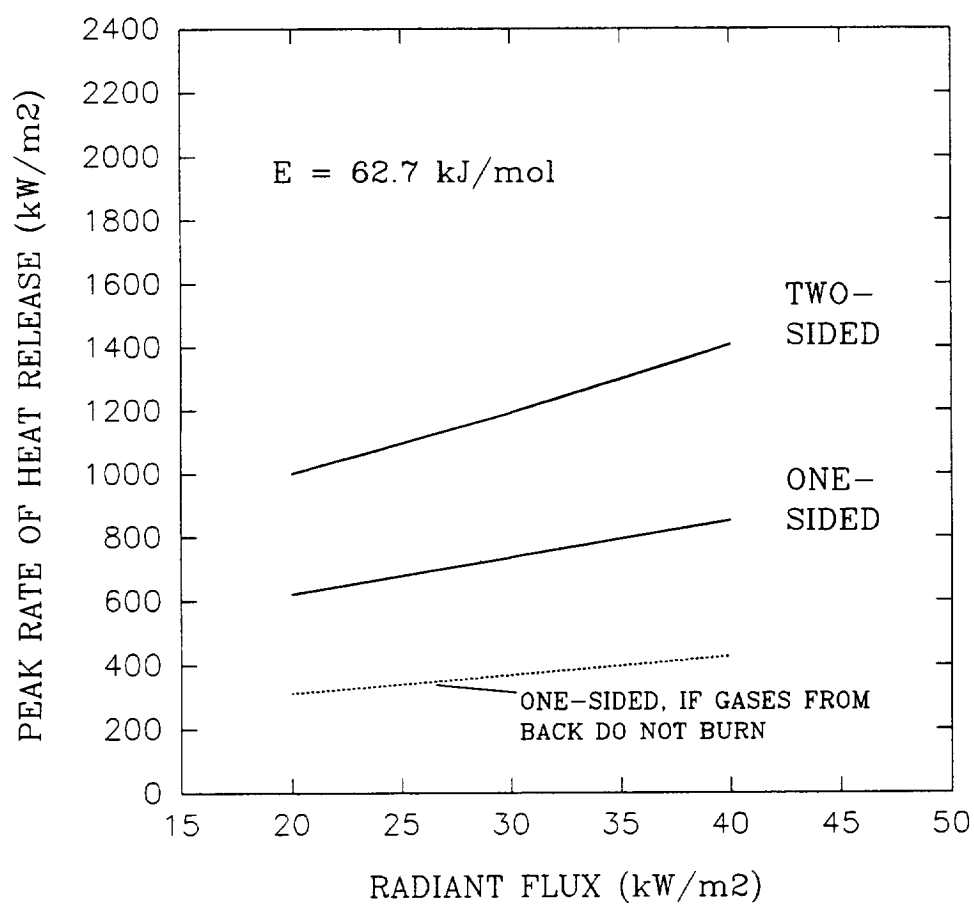


FIGURE 6
TRANSIENT MODEL RESULT
ONE-SIDED AND TWO-SIDED HEATING/BURNING



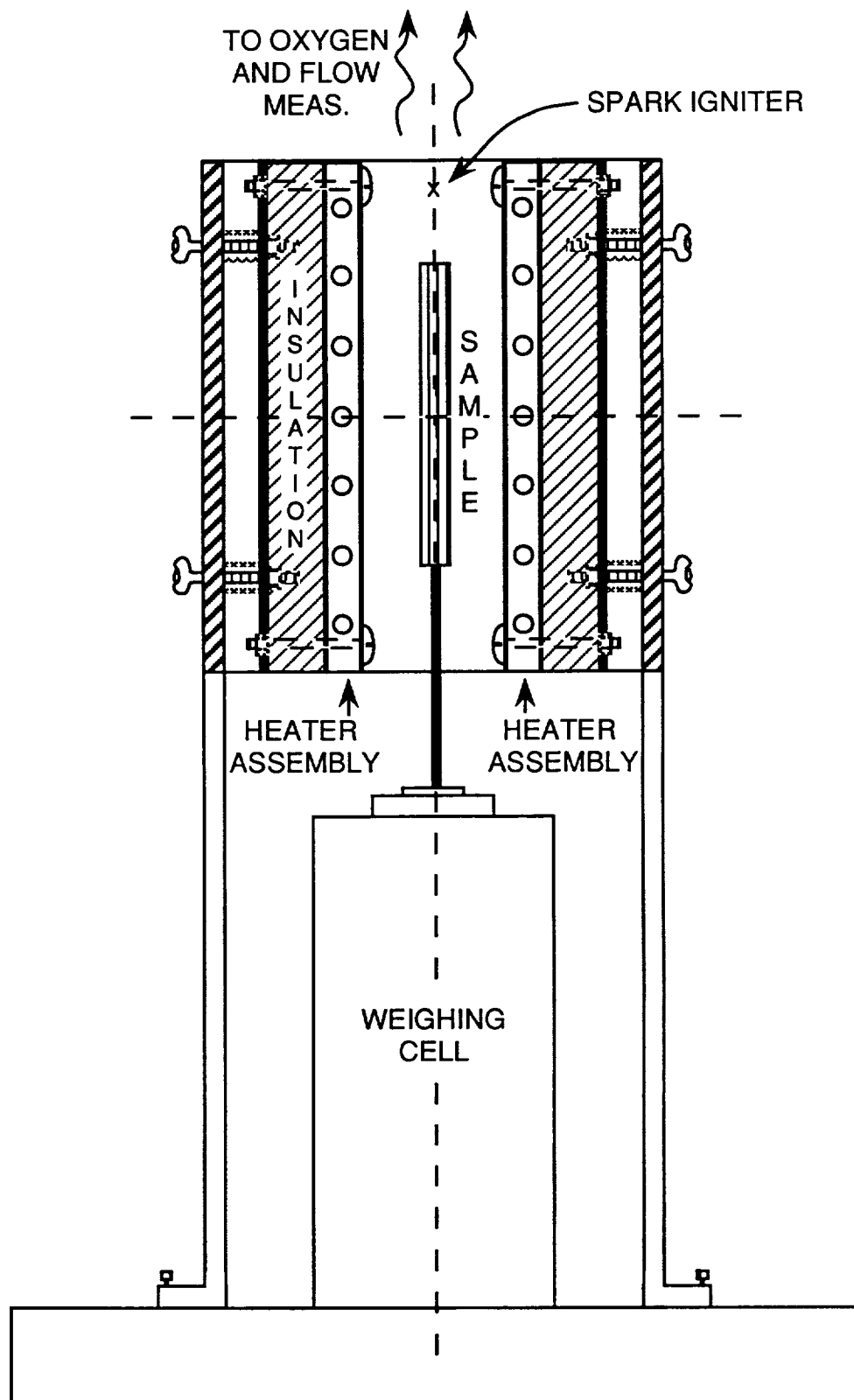


FIG. 7 APPARATUS FOR ONE AND TWO - SIDED BURNING OF SAMPLES IN THE CONE CALORIMETER.

Haysite H755

One-sided Irradiance at 18 kW/m^2

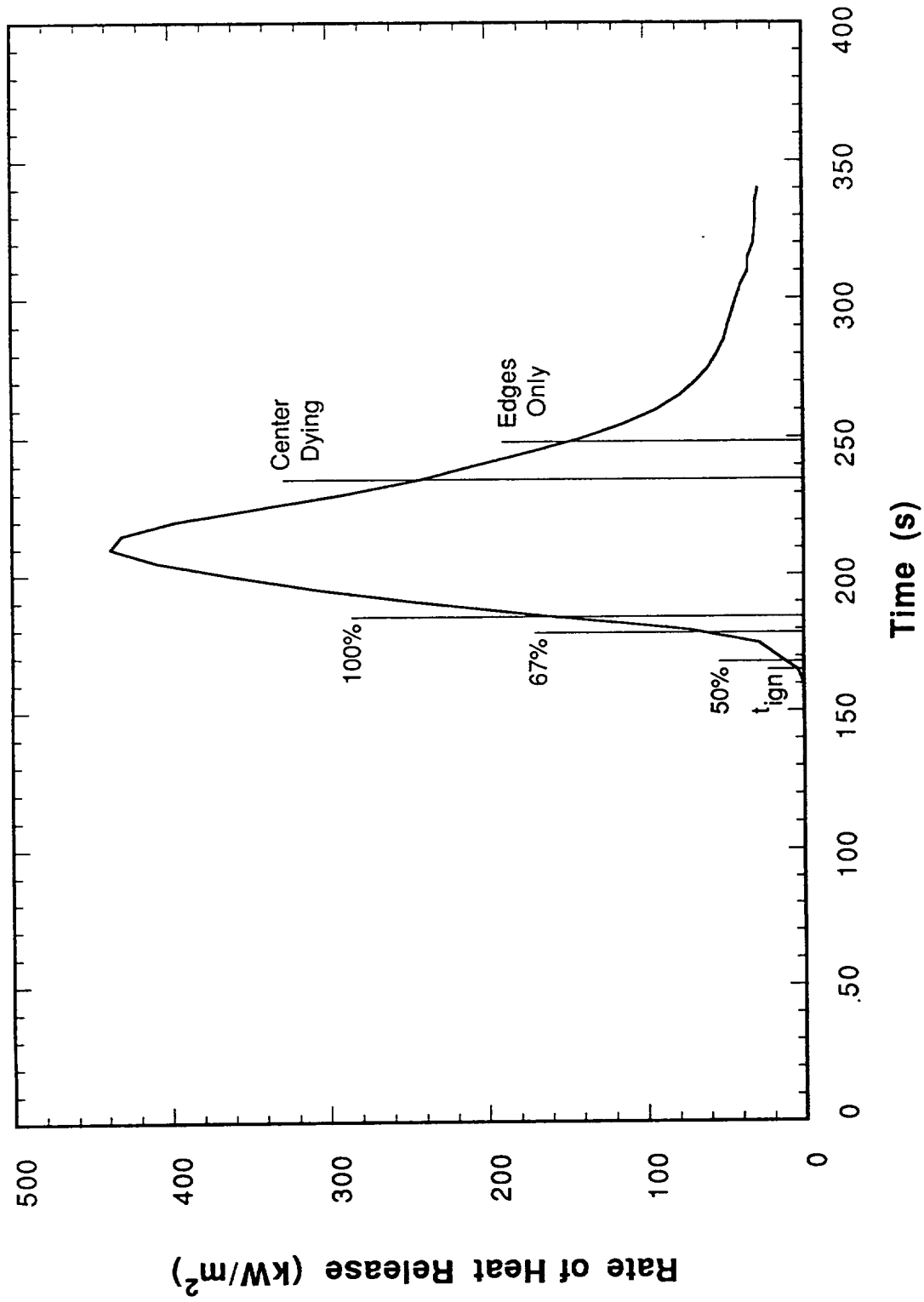


Fig. 8 Typical experimental rate of heat release curve showing percent of sample face area which is burning, as well as events in the dying out of the burning process. "Center Dying" is the earliest indication that the flame near the center of the sample face was going out.

FIGURE 9
ONE-SIDED AND TWO-SIDED RATE OF HEAT RELEASE
G-11 EPOXY/GLASS, 1.5 mm THICK

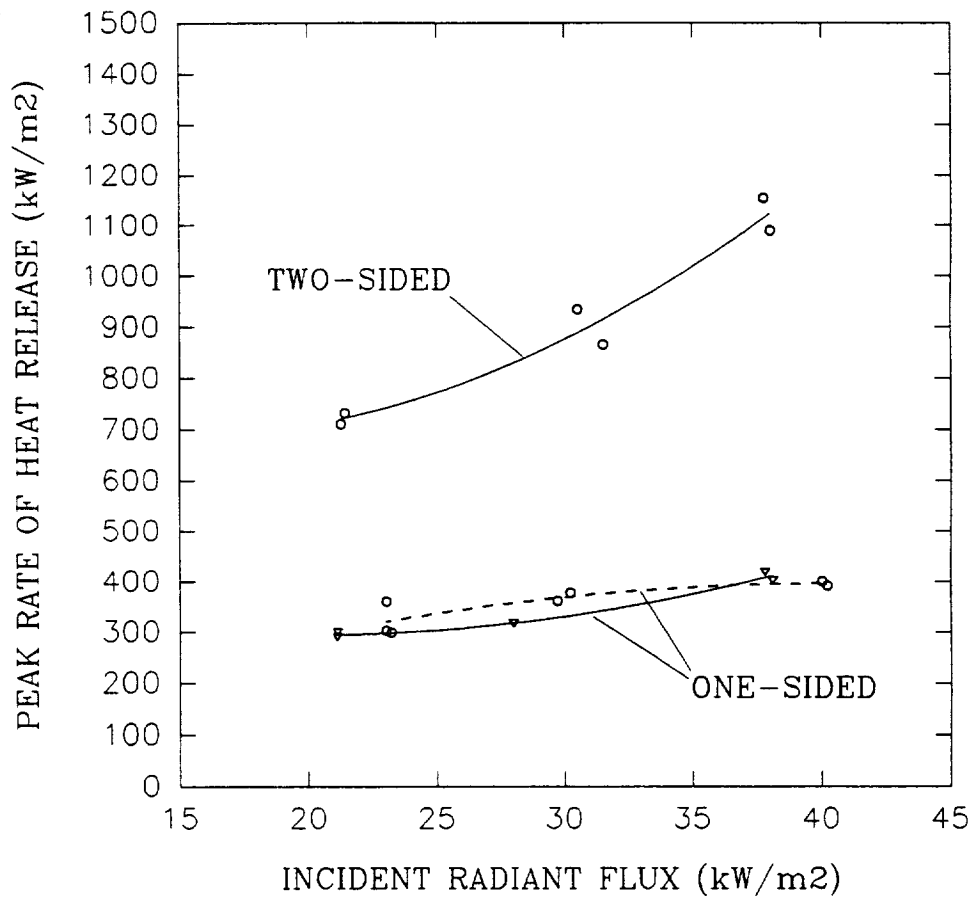


FIGURE 10
ONE-SIDED AND TWO-SIDED RATE OF HEAT RELEASE
HAYSITE H755 POLYESTER/GLASS, 1.5 mm THICK

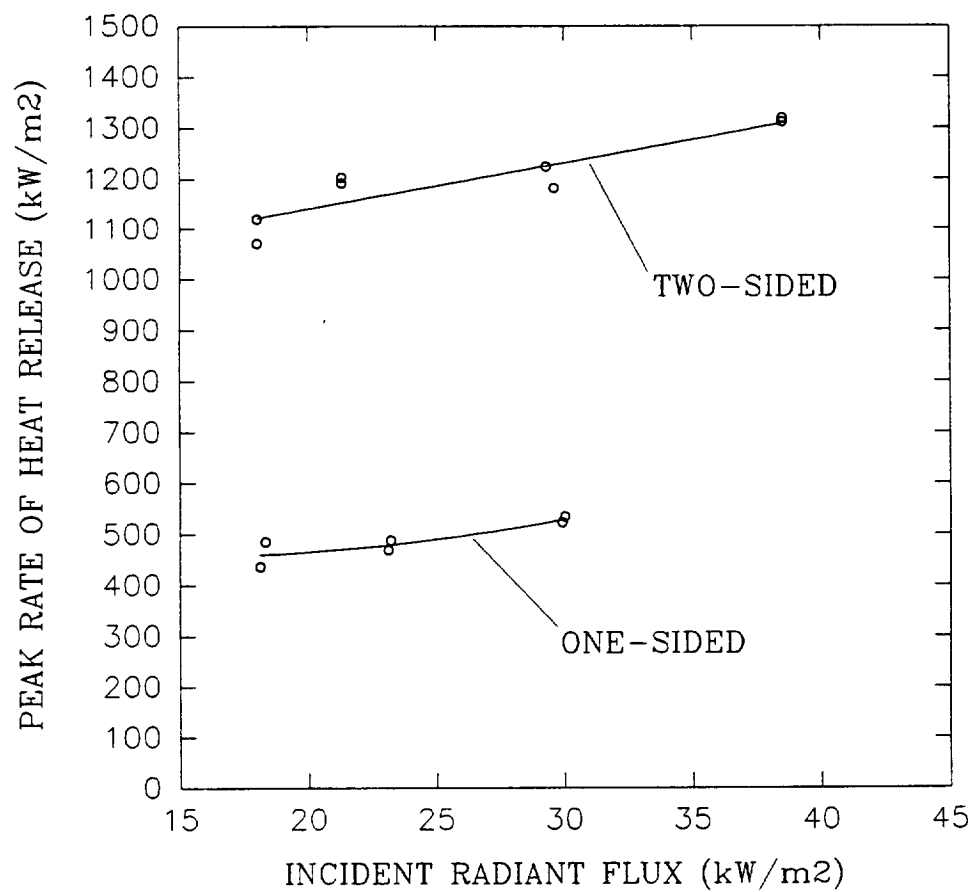


FIGURE 11

ONE-SIDED AND TWO-SIDED RATE OF HEAT RELEASE
HAYSITE ETS POLYESTER/GLASS, 1.5 mm THICK

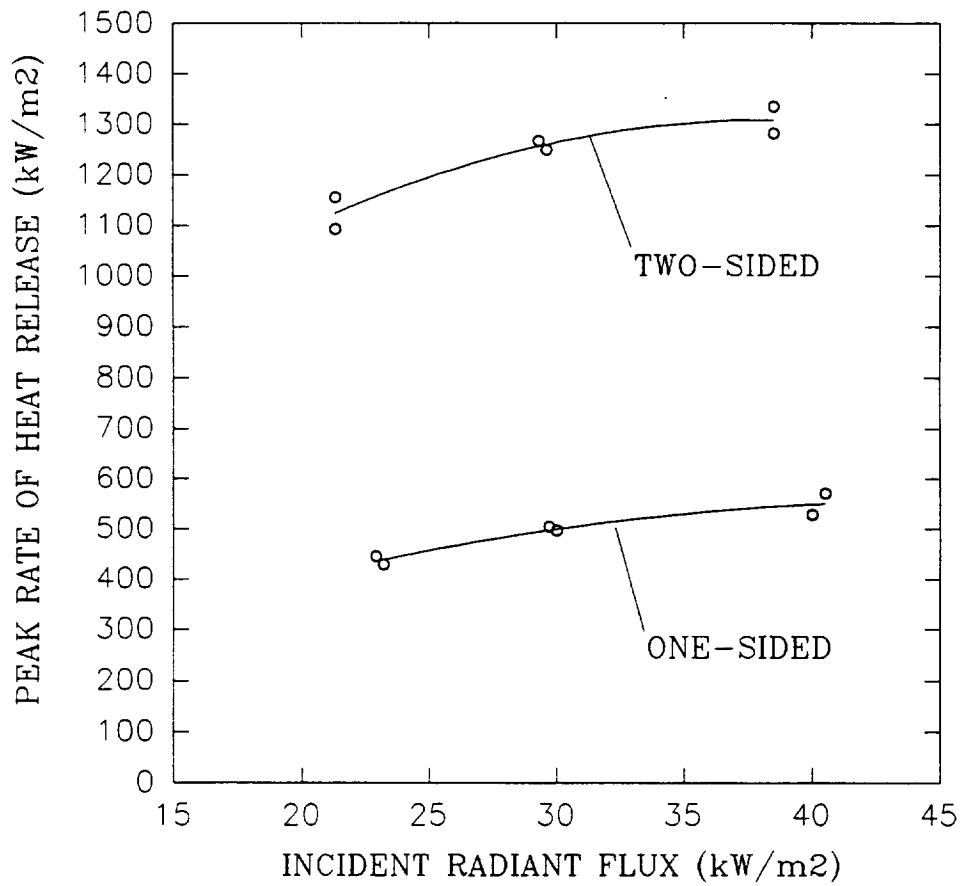


FIGURE 12

CENTERLINE VIEW FACTOR DEPENDENCE ON
RATIO OF SOURCE SIZE TO GAP WIDTH

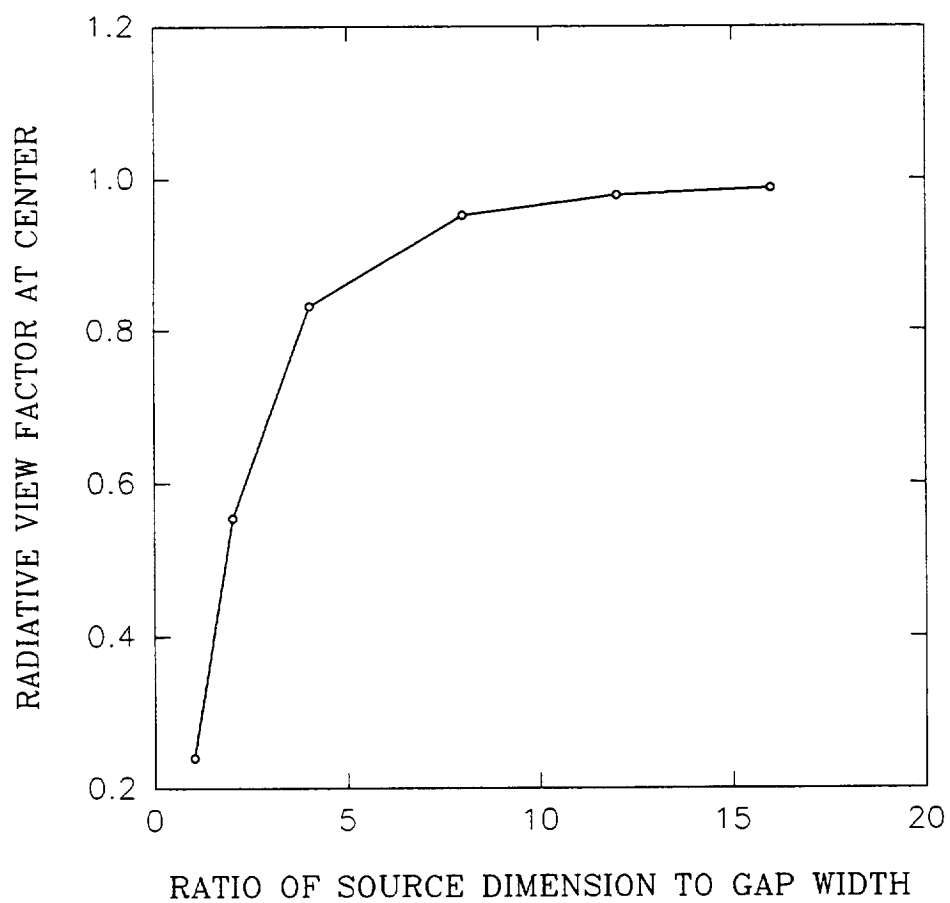
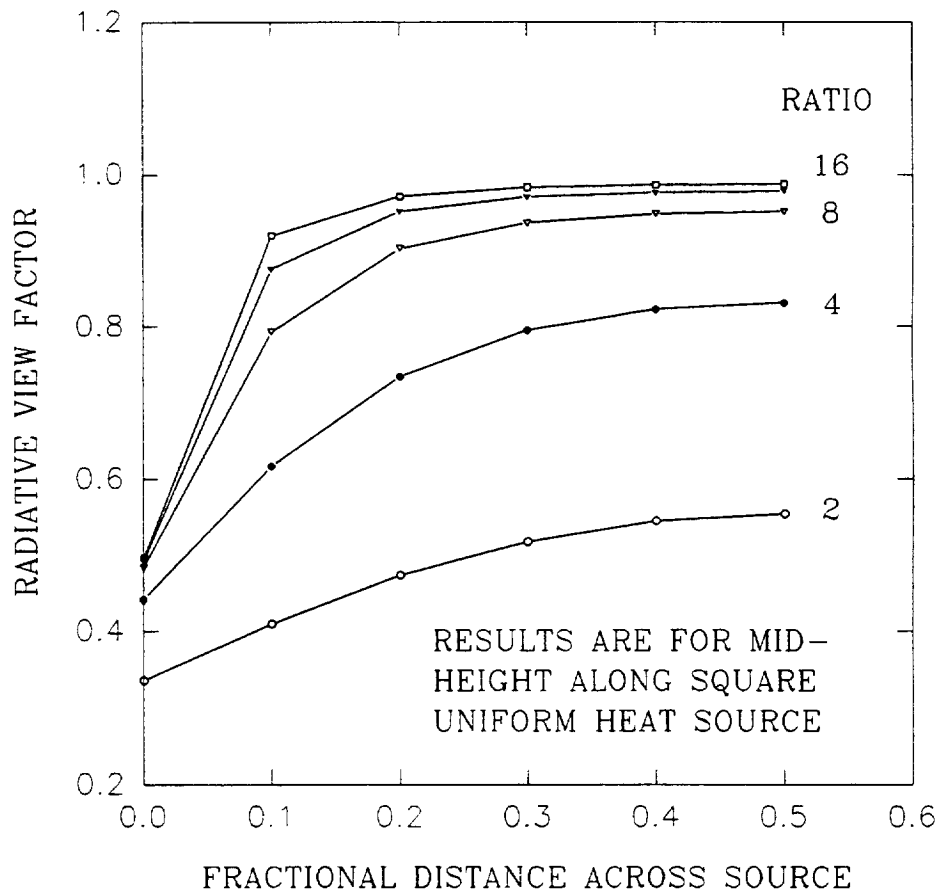


FIGURE 13
VARIATION OF LOCAL VIEW FACTOR
WITH RATIO OF SOURCE WIDTH TO GAP



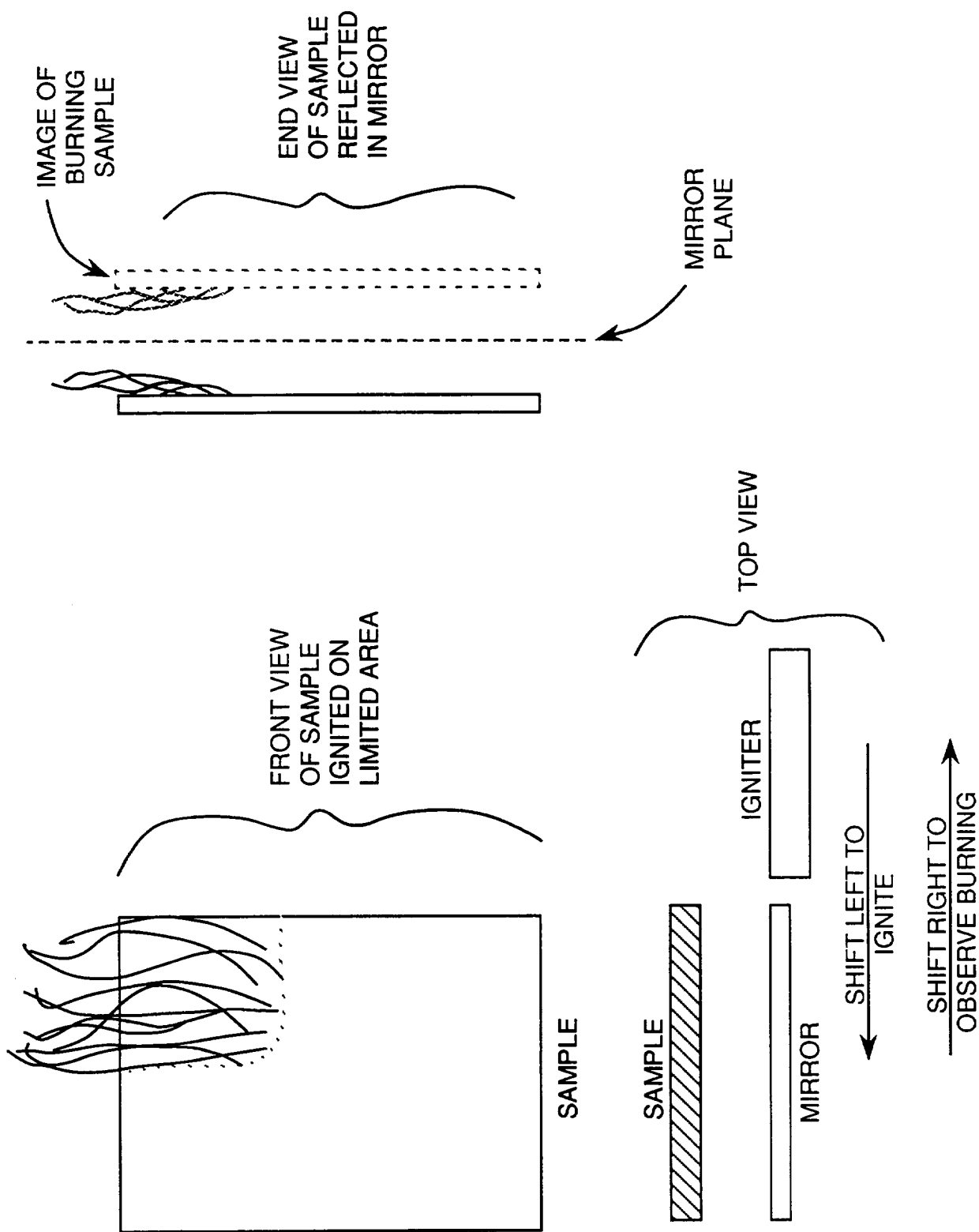


FIG. 14 ELEMENTS OF APPARATUS TO EXAMINE RADIATION SELF-FEEDBACK EFFECT ON OPPOSED - FLOW FLAME SPREAD

NIST-114A (REV. 3-90)		U.S. DEPARTMENT OF COMMERCE NATIONAL INSTITUTE OF STANDARDS AND TECHNOLOGY		1. PUBLICATION OR REPORT NUMBER NASA CR-189226
BIBLIOGRAPHIC DATA SHEET		2. PERFORMING ORGANIZATION REPORT NUMBER NISTIR 4882		
		3. PUBLICATION DATE August 1992		
4. TITLE AND SUBTITLE An Assessment of the NASA Flammability Screening Test and Related Aspects of Material Flammability				
5. AUTHOR(S) T. J. Ohlemiller				
6. PERFORMING ORGANIZATION (IF JOINT OR OTHER THAN NIST, SEE INSTRUCTIONS) U.S. DEPARTMENT OF COMMERCE NATIONAL INSTITUTE OF STANDARDS AND TECHNOLOGY GAITHERSBURG, MD 20899		7. CONTRACT/GRANT NUMBER C-32003-R		
		8. TYPE OF REPORT AND PERIOD COVERED Final Report; 7/89-6/92		
9. SPONSORING ORGANIZATION NAME AND COMPLETE ADDRESS (STREET, CITY, STATE, ZIP) NASA Lewis Research Center Cleveland, OH 44135				
10. SUPPLEMENTARY NOTES				
11. ABSTRACT (A 200-WORD OR LESS FACTUAL SUMMARY OF MOST SIGNIFICANT INFORMATION. IF DOCUMENT INCLUDES A SIGNIFICANT BIBLIOGRAPHY OR LITERATURE SURVEY, MENTION IT HERE.) <p>This final report summarizes the results of an assessment of the NASA flammability screening test (8060.1B) for materials to be used in manned spacecraft interiors. A set of materials was examined using the standard NASA test, a modified version of this test which incorporated external radiation and NIST tests which measure ignitability, rate of heat release and opposed flow flame spread behavior. Materials passing the standard NASA screening test showed widely varying degrees of flammability enhancement when subjected to external radiation (modified NASA test, NIST tests). Since such radiation is implicit in many normal fire scenarios, materials passing the standard NASA screening test should not be treated as non-flammable. The quantitative role of self-feedback of radiation remains to be fully clarified; an apparatus to examine this issue was built but no tests could be completed in the allotted time. The rate of heat release from the two-sided burning of thermally-thin materials was quantitatively compared to that for one-sided burning; this issue was believed to be at the heart of certain anomalies in the earlier stages of this study. A synergistic enhancement of heat release rate was indeed found for two-sided burning of three materials; two simplified models account for the origin of this effect. On the basis of this study, it is recommended that NASA supplement their existing flammability screening test with one that incorporates external radiation. It is further recommended that this supplemental test in normal gravity be correlated experimentally with a similar test in micro-gravity.</p>				
12. KEY WORDS (6 TO 12 ENTRIES; ALPHABETICAL ORDER; CAPITALIZE ONLY PROPER NAMES; AND SEPARATE KEY WORDS BY SEMICOLONS) fire safety; fire tests; flame spread; flammability; heat release rate; ignitability; microgravity; spacecraft fires.				
13. AVAILABILITY <input checked="" type="checkbox"/> UNLIMITED <input type="checkbox"/> FOR OFFICIAL DISTRIBUTION. DO NOT RELEASE TO NATIONAL TECHNICAL INFORMATION SERVICE (NTIS). <input type="checkbox"/> ORDER FROM SUPERINTENDENT OF DOCUMENTS, U.S. GOVERNMENT PRINTING OFFICE, WASHINGTON, DC 20402. <input checked="" type="checkbox"/> ORDER FROM NATIONAL TECHNICAL INFORMATION SERVICE (NTIS), SPRINGFIELD, VA 22161.			14. NUMBER OF PRINTED PAGES 45	
			15. PRICE A03	

ELECTRONIC FORM

